Available online at www.sciencedirect.com
ScienceDirect
Journal of Magnetic Resonance 192 (2008) 48–59
JMR Journal of Magnetic Resonance
www.elsevier.com/locate/jmr

^2H_2O quadrupolar splitting used to measure water exchange in erythrocytes

Philip W. Kuchel *, Christoph Naumann

School of Molecular and Microbial Biosciences, University of Sydney, Building G08, NSW 2006, Australia

Received 13 April 2007; revised 14 January 2008
Available online 1 February 2008

Abstract

The ^2H NMR resonance from HDO ($D = {}^2H$) in human red blood cells (RBCs) suspended in gelatin that was held stretched in a special apparatus was distinct from the two signals that were symmetrically arranged on either side of it, which were assigned to extracellular HDO.

The large extracellular splitting is due to the interaction of the electric quadrupole moment of the ^2H nuclei with the electric field gradient tensor of the stretched, partially aligned gelatin. Lack of resolved splitting of the intracellular resonance indicated greatly diminished or absent ordering of the HDO inside RBCs. The separate resonances enabled the application of a saturation transfer method to estimate the rate constants of transmembrane exchange of water in RBCs. However both the theory and the practical applications needed modifications because even in the absence of RBCs the HDO resonances were maximally suppressed when the saturating radio-frequency radiation was applied exactly at the central frequency between the two resonances of the quadrupolar HDO doublet.

More statistically robust estimates of the exchange rate constants were obtained by applying two-dimensional exchange spectroscopy (2D EXSY), with back-transformation analysis. A monotonic dependence of the estimates of the efflux rate constants on the mixing time, t_{mix}, used in the 2D EXSY experiment were seen. Extrapolation to $t_{mix} = 0$, gave an estimate of the efflux rate constant at 15 °C of $31.5 \pm 2.2\ s^{-1}$ while at 25 °C it was $\sim 50\ s^{-1}$. These values are close to, but less than, those estimated by an NMR relaxation-enhancement method that uses Mn^{2+} doping of the extracellular medium. The basis for this difference is thought to include the high viscosity of the extracellular gel.

At the abstract level of quantum mechanics we have used the quadrupolar Hamiltonian to provide chemical shift separation between signals from spin populations across cell membranes; this is the first time, to our knowledge, that this has been achieved.

Keywords: ^2H NMR; Aligned media in NMR; Erythrocytes; Red blood cells; Residual quadrupolar splitting; Water transport

1. Introduction

Water transport across the plasma membrane of the human erythrocyte (red blood cell; RBC) is very rapid with the mean residence time of a water molecule in the cell being ~10 ms at 37 °C [1]; this implies that the total water contents turn over ~100 times a second [2]. The exchange is mediated by the ~200,000 copies of aquaporin 1 that reside in the plasma membrane [2]. The most versatile method for measuring this exchange, under diverse conditions, including in the presence of reagents that inhibit the process, is NMR spectroscopy; the method of choice involves 'doping' the medium around the cells with Mn^{2+}; this greatly reduces the T_2 of water outside the cells relative to inside. Then transverse relaxation time courses are recorded using a ^1H NMR Carr-Purcell-Meiboom-Gill (CPMG) pulse sequence e.g., [3,4]; and the bi-exponential relaxation time course is fitted by regression analysis using a 2-site exchange model to obtain an estimate of the efflux rate

Abbreviations: 2D EXSY, two dimensional exchange spectroscopy; 2D NOESY, two dimensional nuclear Overhauser spectroscopy; CPMG, Carr-Purcell-Meiboom-Gill; HDO, deuterated water; PGSE, pulsed field gradient spin echo; RBC, red blood cell

* Corresponding author. Fax: +61 2 9351 4726.
E-mail address: p.kuchel@mmb.usyd.edu.au (P.W. Kuchel).

1090-7807/$ - see front matter © 2008 Elsevier Inc. All rights reserved.
doi:10.1016/j.jmr.2008.01.010

constant [5]. Alternatively, the different rates of translational diffusion of water inside and outside RBCs can be used with Kärger's 2-site analysis [6], based on pulsed field gradient spin echo (PGSE) spectra, to estimate the value of the efflux rate constant e.g., [7,8].

Other less direct NMR-based methods rely on fitting a function to the spectral line-shape [9]; but with water these methods are complicated by the rapidity of the exchange and the inability to obtain reproducible extents of transmembrane differences in magnetic susceptibility [10–15]. Attempts to use paramagnetic shift reagents to bring about the separation of the water resonances for inside and outside the cells are also thwarted by the rapidity of the exchange [10,11].

We reasoned that if separate signals could be obtained from water by some other means than shift reagents then the robust and well-tried analytical methods of magnetization transfer might be useful; such methods include saturation transfer [16,17]. This methodology would obviate the need to add low molecular weight reagents to the cell suspensions that could potentially interfere with the mechanisms under study.

We recently described a device in which liquid gelatin is drawn into a silicone-rubber tube that is then sealed at its lower end; the tube is inserted into a bottomless 5- or 10-mm NMR tube [18]. Upon setting of the gel a plastic thumbscrew is tightened at the top end of the glass tube to hold the silicone tube and gelatin at various extents of stretching. It is notable that RBCs can be incorporated into the gel and their properties studied in their stretched state. Since gelatin is a biopolymer-protein made from L-amino acids it has the additional ability to resolve the spectra of enatiomeric pairs of compounds such as L/D-alanine [19].

In the present paper we report on the ability to separate the NMR resonances of water inside and outside RBCs in suspensions. This exploits the spectral splitting that is brought about by the interaction between the electric quadrupole moment of the ^{2}H nucleus in HDO and the electric field gradient tensor of gelatin molecules, when they are partially aligned with the main magnetic field by stretching the gel. Moreover, although RBCs embedded in stretched gelatin are also stretched, the cytoplasm and cytoskeleton appear not to impose order on HDO to anywhere near the same extent, as the ^{2}H NMR spectrum of a suspension of RBCs in stretched gelatin shows only three resonances, two from the HDO outside, and one between these from HDO inside (Fig. 1). Note that we used a mixture of ^2H_2O and ^1H_2O that was typically between 20% and 100% ^2H_2O so we denote the solvent as HDO, where D is the alternative symbol for deuterium.

This spatial dependence of the chemical shift of HDO enabled the application of two magnetization transfer methods, saturation transfer, and two-dimensional exchange spectroscopy (2D EXSY), to estimate the efflux rate constant for transmembrane exchange; this is a kinetic parameter that is of special interest to cell biologists e.g., [2]. And in the context of quantum mechanics, previous NMR methods that are used to measure membrane transport in cells have exploited the Zeeman Hamiltonian, but this new method uses the quadrupolar Hamiltonian.

2. Methods

2.1. Theory

2.1.1. Magnetization transfer—general

NMR magnetization transfer experiments, including the saturation transfer method, are widely used to measure the rate of exchange between two *chemically* distinct species in a system that is at equilibrium, but undergoing rapid 'tracer exchange' e.g., [16,17]. The relevant theory also enables an estimate of influx or efflux rate constants for membrane transport systems that do not involve chemical *transformation* but spatial *translocation* i.e., transport between compartments where there are differences in chemical shift brought about by environmental factors. The basic theory has been presented for saturation transfer analysis [16,17] and has been adapted into a two-dimensional method, 2D EXSY e.g., [20], and a time-efficient one-dimensional counterpart, 1D EXSY [21]. The pulse sequence used is identical to the 2D nuclear Overhauser spectroscopy (2D NOESY) experiment, namely delay-$\pi/2 - t_1 - \pi/2 - t_{mix} - \pi/2$-acquire.

2.1.2. Saturation transfer—modified

While the basic theory has been presented before [17] some extensions are required to handle the present case so a brief summary is necessary: a 2-site system exchanging between a pool, E, and another one, I, is written as:

$$E \underset{k_{-1}}{\overset{k_1}{\leftrightarrow}} I \tag{1}$$

and the Bloch–McConnell [22] equations that describe the time dependence of magnetization in a simple pulse-acquire NMR experiment are:

$$\begin{aligned}\frac{\mathrm{d}}{\mathrm{d}t}M_z^E &= -\left(\frac{M_z^E - M_{z,eq}^E}{T_1^E}\right) - k_1 M_z^E + k_{-1} M_z^I \\ \frac{\mathrm{d}}{\mathrm{d}t}M_z^I &= -\left(\frac{M_z^I - M_{z,eq}^I}{T_1^I}\right) + k_1 M_z^E - k_{-1} M_z^I - k_{sat} M_z^I\end{aligned} \tag{2}$$

where, respectively, M_z^E and M_z^I denote the magnetizations of the spin populations E, and I; $M_{z,eq}^E$ and $M_{z,eq}^I$ are the equilibrium magnetizations; T_1^E and T_1^I are the longitudinal relaxation times; and k_1 and k_{-1} are the forward and reverse rate constants that characterize the exchange reaction. *In addition* we include the term, $k_{sat}\, M_z^I$ to describe the rate of loss of I-magnetization brought about by selectively irradiating the sample at the absorption frequency of the I spins, where k_{sat} is a first-order rate constant, the value of which depends on the power of the radio-frequency (RF) irradiation field.

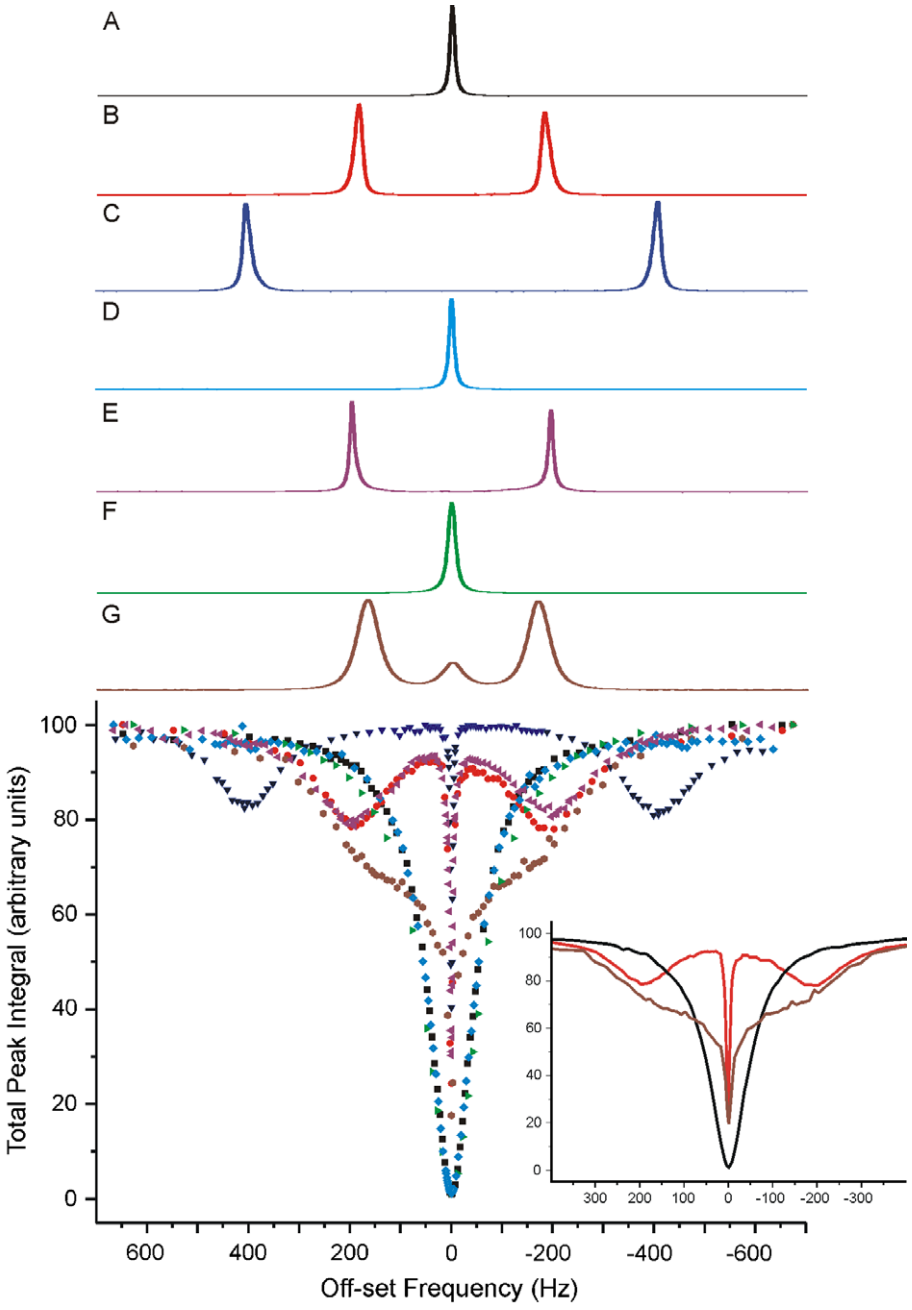

Fig. 1. ^{2}H NMR (61.422 MHz) spectra of stretched and unstretched gelatin gels and the effect of applying selective RF irradiation to the ^{2}H spins. The graph shows the effect of changing the off-set frequency of the applied RF radiation on the total ^{2}H NMR signal intensity (integral) of HDO, while the corresponding starting spectra were obtained without any selective irradiation. The sample of gelatin was prepared from 50% (w/v) bovine gelatin with 100% (v/v) $^{2}H_2O$. (A) ^{2}H NMR spectrum with the gel in the unstretched state; and in the graph (called the *saturation envelope*) the black squares show the total integral of the two signals obtained from this sample with RF radiation of fixed power applied at the specified off-set frequencies. (B) Spectrum obtained after the gel in A was stretched to 1.6 times it original length; and the red discs in the graph define its corresponding saturation envelope. (C) Spectrum obtained after the gel in A was stretched to 2.3 times its original length; and the dark blue triangles in the graph define its corresponding saturation envelope. (D) Spectrum obtained after the gel was melted while the silicone tube remained stretched, and then the sample was cooled again to 15 °C; and the blue diamonds in the graph define its corresponding saturation envelope. (E) Spectrum obtained from the sample in D, after the silicone tube was released thus compressing the gel; and the purple triangles in the graph define its corresponding saturation envelope. (F) Spectrum obtained from the sample that contained gelatin and human RBCs; and the green triangles in the graph define its corresponding saturation envelope. (G) Spectrum obtained from the sample in F but stretched to twice its original length; and the brown hexagons in the graph define its corresponding saturation envelope. The gel containing RBCs (sample 5 in Table 1, spectra F and G) was prepared from 30% (w/v) bovine gelatin samples with 20% (v/v) $^{2}H_2O$ in aqueous saline (154 mM NaCl, 10 mM glucose), containing a final *Ht* of 19%. The temperature for all spectra was 15 °C. NMR parameters: pulse sequence was delay-$\pi/2$-acquire with RF saturating power applied in the delay period of 1 s; the power was chosen so as to fully suppress the ^{2}H signal when directly on resonance with the unstretched gel (50 dB from a 300 W amplifier); spectra were acquired with the radiation off-set moved in steps of 5–25 Hz as shown; $\pi/2$ pulse duration was 33.5 ms at 2 dB attenuation; number of transients per spectrum was 32; and the total acquisition time per spectrum was 0.5 min.

We seek an expression that gives k_1 or k_{-1} as a function of experimentally determined or specified values viz., $M^E_{z,eq}$, T^E_1 etc. This is done as follows: In a *chemically* exchanging system (not a membrane transport one) it is *not* usually possible to measure separately the value of T^E_1 or T^I_1 because the exchange process, whose rate is as yet unknown from the experiment, enhances the overall rate. Instead, the longitudinal relaxation of M^E_z is measured while saturating the I spin-population giving an estimate of the parameter called $T^{E,sat}_1$ [16,17]:

$$T^{E,sat}_1 = \frac{T^E_1}{1 + k_1 T^E_1} \tag{3}$$

The saturation transfer experiment is carried out by selectively irradiating the I-spin population with sufficient RF power to saturate its magnetization. Under conditions of steady state of magnetization, this amounts to setting the left-hand side of the two equations in Eq. (2) to 0, and setting $M^I_z = 0$. Experimentally, the signal from E is reduced, corresponding to a smaller value, $M^E_{z,sat}$. A separate spectrum acquired without the saturating RF field yields the value of $M^E_{z,eq}$. Hence the decrease in signal is proportional to $(M^E_{z,eq} - M^E_{z,sat}) = \Delta M^E_z$; and by rearranging Eq. (2), and using Eq. (3) the expression for k_1 becomes:

$$k_1 = \left(\frac{\Delta M^E_z}{M^E_{z,eq}}\right)\frac{1}{T^{E,sat}_1} \tag{4}$$

In the case of cell-membrane transport it is often possible to measure directly the T_1 in either compartment by separating the cells by centrifugation. In this case another version of Eq. (4) is obtained [23]:

$$k_1 = \frac{1}{\frac{1}{\left(\frac{\Delta M^E_z}{M^E_{z,eq}}\right)} - 1}\frac{1}{T^E_1} \tag{5}$$

where the awkward-looking nested reciprocal is used to retain the ratio of the change in magnetization to the equilibrium value, as in Eq. (4).

With cell-membrane transport the *extrinsic* equilibrium constant, K_{eq}, is measured from the NMR spectrum as the ratio of the resonance integrals:

$$k_{eq} = \frac{M^I_{z,eq}}{M^E_{z,eq}} = \frac{k_1}{k_{-1}} \tag{6}$$

If, as was the case in the present study, it is not experimentally possible to fully saturate the magnetization of the I spin-population a residual term, $M^I_{z,sat}$, appears in Eq. (2) at steady state. Then the expression for k_1 is obtained, after rearranging Eq. (6):

$$k_1 = \frac{\Delta M^E_z}{M^E_{z,eq}}\frac{1}{T^E_1}\frac{1}{(\alpha - \beta)} \tag{7}$$

or

$$k_1 = \frac{1}{T^E_1}\left(\frac{1-\alpha}{\alpha - \beta}\right) \tag{8}$$

where

$$\alpha = \frac{M^E_{z,sat}}{M^E_{z,eq}} \text{ and } \beta = \frac{M^I_{z,sat}}{M^I_{z,eq}} \tag{9}$$

It is expedient to relate k_1 to the efflux rate constant: for an electrically neutral chemical species like water its transmembrane distribution is virtually thermodynamically 'ideal'; although there are subtle chemical shift effects that clearly reveal that the water activity inside an RBC is not 1.0 [13–15]. But, to an excellent approximation here, the K_{eq} value is simply the ratio of the resonance areas that in turn is proportional to the ratio of the cell-water volume to the extracellular volume.

Finally, the mean residence lifetime for exchange, τ_e, for water inside the cells is simply given by $1/k_{-1}$, and from Eq. (6) it is:

$$\tau_e = \left(\frac{M^I_{z,eq}}{M^E_{z,eq}}\right)\frac{1}{k_1} = \frac{K_{eq}}{k_1} \tag{10}$$

2.1.3. 2D-EXSY

The Bloch–McConnell equations for a 2-site exchange system can also be solved in a general and compact way by using a matrix method e.g., [20] such that the form of the input and output is clearly connected to the data from a 2D EXSY spectrum. Hence for a 2-site exchange scheme the so-called exchange matrix is [20]:

$$\mathbf{R} = -\begin{bmatrix} \frac{1}{T^E_1} + k_1 & -k_{-1} \\ -k_1 & \frac{1}{T^I_1} + k_{-1} \end{bmatrix} \tag{11}$$

where, T^E_1 and T^I_1 are the longitudinal relaxation times of the extra- and intracellular HDO. The analysis uses estimates of the resonance volumes of as 2D EXSY spectrum, expressed as the matrix, $\mathbf{M}$, for a specified mixing time, t_{mix}, and the diagonal resonance volumes of the spectrum $\mathbf{M}_0$, when $t_{mix} = 0$. $\mathbf{M}_0$ is often conveniently obtained from a one-dimensional spectrum that is converted from the vector $\mathbf{S}_0$ into a diagonal matrix while α is a scaling factor that does not need to be evaluated if only the ks and not the T_1s are sought [20]:

$$\mathbf{M}_0 = \alpha\mathbf{S}_0 \tag{12}$$

The analysis proceeds by taking the matrix product of $\mathbf{M}$ and the inverse of $\mathbf{M}_0$ and extracting the diagonal eigenvector matrix, $\mathbf{\Lambda}$, and its corresponding eigenvalue matrix, $\mathbf{U}$:

$$\mathbf{M}\cdot\mathbf{M}_0^{-1} = \mathbf{U}\cdot\mathbf{\Lambda}\cdot\mathbf{U}^{-1} \tag{13}$$

This is a routine numerical procedure in programs like *Mathematica* [24], which was used here; but judicious use was made of the Transpose function to achieve the correct output. The natural logarithm of both elements of $\mathbf{\Lambda}$ are

taken, and the matrix product is reformed, multiplied by $(1/t_{mix})$ and the off-diagonal elements of the 2×2 matrix $\mathbf{R}'$ are the respective estimates of k_{-1} and k_1:

$$\mathbf{R}' = (1/t_{mix})\mathbf{U} \cdot \mathrm{Ln}(\mathbf{\Lambda}) \cdot \mathbf{U}^{-1} \quad (14)$$

Estimates of errors in parameters within one experiment can be made by using the signal-to-noise ratio in the $\mathbf{M}$ and $\mathbf{M}_0$ spectra [20], but experience shows that inter-experiment variation is much higher than this; hence in the results below the errors are based on replicated experiments.

Finally, as in Eq. (10) the value of the mean residence time of water in an RBC, τ_e, is given by $1/k_{-1}$.

2.2. RBC preparation

Blood was obtained by venipuncture in the cubital fossa from healthy donors with University of Sydney Human Ethics Committee consent. The cells were prepared by three-fold washing by centrifugation at 3000*g* at 4 °C in ~4 volumes of physiological saline (0.154 M NaCl) constituted in 20–100% ^2H_2O. The cell suspension was bubbled with CO before the last centrifugation step to stabilize the hemoglobin in its diamagnetic state e.g., [13]. Cell packing density or hematocrit (*Ht*) values were measured by capillary centrifugation (Clements, North Ryde, NSW, Australia) [25].

2.3. Gelatin preparation

Gelatin gels were made as previously described [18,19]; the gelatin (Gelita grade 20N) was a gift from Gelita (Sydney, NSW, Australia). To help maintain the normal biconcave shape of the RBCs, 0.5% (w/v) defatted bovine serum albumin was included, along with adjustment to pH 7.4. Our typical blood-gelatin preparation was: 3.0 g gelatin mixed with 5.0 mL of pH 7.4 buffer identical to the one used for blood preparation. 100 μL of 5 M NaOH was added (this amount added to 3.0 g of gelatin in 20 mL of water gave pH 7.4). The mixture was heated to 65 °C, and stirred twice, until a clear and bubble free solution was formed. The gel was cooled to 42 °C, and 5 mL of RBC suspension of *Ht* ~80% was added. The blood-gelatin mixture was gently stirred and left to equilibrate for 30 min at no more than 42 °C before preparing the NMR samples.

2.4. Gel stretching

Liquid gelatin solutions (30–50% w/v) with or without RBCs suspended (*Ht* ~ 15–30%) were drawn into silicone-rubber tubes (2.0 or 6.5 mm i.d.; Sims Portex, Hythe, Kent, UK). The tube was then placed into a thick-walled glass tube 190-mm long with an o.d., of 10 mm, or 180-mm long with an o.d., of 5 mm; the tube was sealed at one end with a rubber stopper for 10-mm samples and a custom made Delrin plug for 5-mm samples. The rubber stopper was trimmed to leave ~3 mm projecting from the base of the glass tube. Each sample was cooled to 15 or 25 °C to enable gelation. When the silicone tube containing the gel was stretched, it was held extended with a plastic thumbscrew at the upper end of the glass tube [18].

2.5. NMR

^{2}H NMR spectra were recorded at 61.422 MHz on a Bruker DRX 400 spectrometer (Bruker Karlsruhe, Germany) with an Oxford Instruments (Oxford, UK) 9.4 T, vertical, wide-bore magnet. ^{1}H NMR spectra were recorded at 400.13 MHz on the same spectrometer. Selective saturation of magnetization at a specified frequency was achieved with a pulse of 1 s duration using a power-attenuation of ~50 dB from the standard Bruker 300 W decoupling amplifier. The actual value of the attenuation factor that was used was adjusted empirically to achieve full signal suppression of the HDO signal in the unstretched state. We varied the irradiation frequencies in small steps throughout the whole spectrum to a frequency for which there was no longer any saturation. After standard 1D processing, all spectra were integrated relative to each other, determining the total area of the signals (Fig. 1). To obtain more specific information the blood gelatin sample were deconvoluted in Topspin 2.0, allowing us to plot separate graphs for the anisotropic (gelatin) and isotropic (blood) parts of the spectra (Fig. 2).

2D EXSY spectra were recorded using the standard 16-step phase cycle with the pulse sequence delay-$\pi/2 - t_1 - \pi/2 - t_{mix} - \pi/2$-acquire. Specific details are given in the relevant figure captions. T_1 values were estimated by using the standard inversion recovery pulse sequence.

Gaussian-Lorentzian deconvolution (Bruker, TopSpin 2.0, release March 21, 2007) or manual integration were used as indicated to extract the relative areas of resonances in 1D spectra, or peak volumes in 2D spectra.

2.6. Data processing

The formation of 2×2 exchange matrices ($\mathbf{M}$) from 3×3 2D EXSY spectra took account of the fact that the two extracellular-HDO resonances represented water in a single extracellular compartment, so their resonance intensities were added together; so too were the pairs of exchange-cross resonances on either side of the leading diagonal in a 2D EXSY spectrum. Hence, the data transformation was as follows, using the standard mathematical row-column notation with the primes denoting the elements of the resulting 2×2 matrix: $\{1,3\} + \{3,3\} \rightarrow \{1',1'\}$; $\{2,3\} + \{3,2\} \rightarrow \{1',2'\}$; $\{1,2\} + \{2,1\} \rightarrow \{2',1'\}$; and $\{2,2\} \rightarrow \{2',2'\}$.

We also used a second method to calculate rate constants from 2D EXSY experiments, the initial rate approximation [26]. At short mixing times, the ratio of cross peak area to diagonal peak area is plotted versus mixing time. The slope represents the particular rate constant, either the forward or back rate constant. Plotting $(\{2,1\} + \{2,3\})/\{2,2\}$ versus t_{mix} would yield k_1 or k_{-1}.

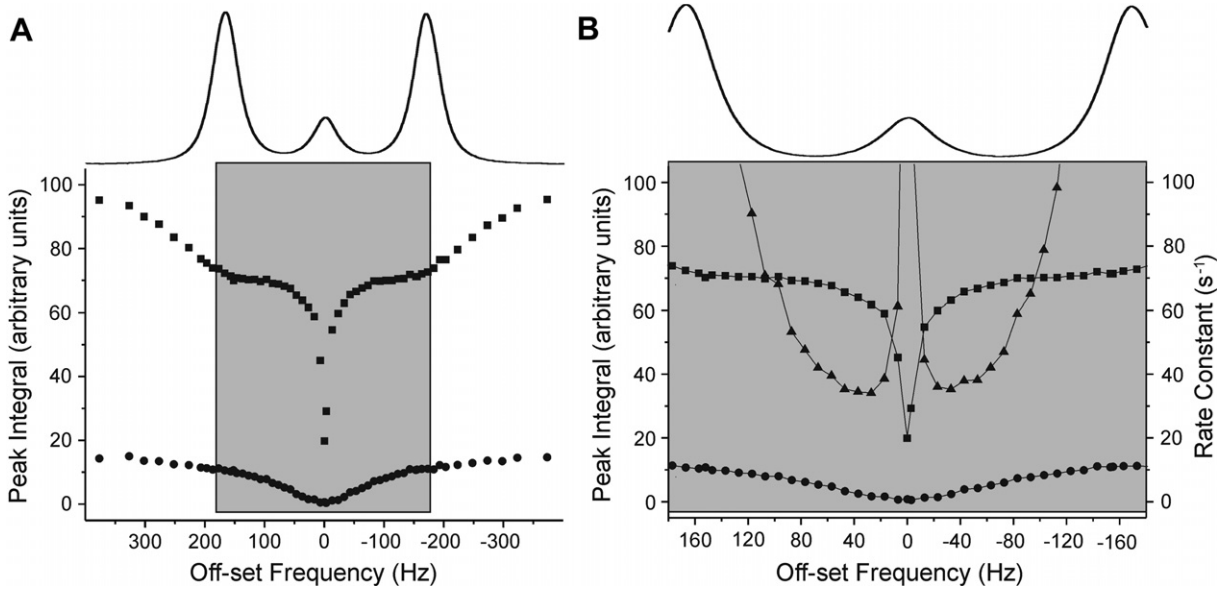

Fig. 2. ^{2}H NMR (61.422 MHz) saturation transfer analysis of water exchange in RBCs in gelatin gel. The sample was stretched to elicit quadrupolar splitting of the extracellular HDO resonance, and the relative peak integrals were obtained by numerical deconvolution (see Section 2.5). (A) ^{2}H NMR spectrum and the corresponding saturation envelopes for the extracellular resonances (solid squares) and the intracellular resonance (solid discs). The grey highlighting delimits areas of data that are shown in (B). (B) Expansion of the spectrum and data in (A) with the additional calculated results of applying Eqs. (6) and (8) to give estimates of k_{-1}. The spectra were acquired from 30% (w/v) bovine gelatin samples with 20% (v/v) ^2H_2O in aqueous saline (154 mM NaCl, 10 mM glucose) with final $Ht = 19\%$. The sample temperature was 15 °C. NMR parameters were the same as for Fig. 1.

Regression analysis, such as that used for Fig. 4, was carried out with Origin Pro Software (OriginLab, Northampton, MA). Standard errors were obtained from the fitting routine.

3. Results

3.1. Quadrupolar splitting of HDO

Fig. 1A shows a typical ^{2}H NMR spectrum of HDO (100% ^2H_2O) in gelatin gel in an unstretched state at 15 °C. The lineshape was Lorentzian and the width-at-half-height, $\Delta\nu_{1/2}$, was 10.4 Hz. This value for duplicate samples was always ~10 Hz. Fig. 1B shows the ^{2}H NMR spectrum obtained under identical conditions to those used for Fig. 1A but the sample was stretched to 1.6 times its original length. The obvious doublet is due to quadrupolar splitting and the value of the residual coupling constant was 366 Hz with $\Delta\nu_{1/2} = 19.3 \pm 0.3$ (range) Hz for each resonance. Overall there was no systematic difference between the $\Delta\nu_{1/2}$ for each of the two quadrupolar signals here and in the subsequent spectra (see Fig. 1B, C, E and G).

Further stretching the gel to 2.3 times its original length gave a quadrupolar spitting of 812 Hz and $\Delta\nu_{1/2} = 17.7$ Hz for each resonance.

With the silicone tube and its enclosed gel in a stretched state (as for Fig. 1C) the tube assembly was heated to 37 °C inside the spectrometer, to melt the gel, and then cooled to 15 °C to allow the gel to reset. Hence, the silicone tube was still stretched but the gel was relaxed. The resulting ^{2}H NMR singlet is shown in Fig. 1D. The sample volume within the region of the receiver-coil volume was less due to it being stretched, so the spectrum was scaled to have the same amplitude as in Fig. 1A. $\Delta\nu_{1/2}$ was 10.7 Hz, which is very close to that of the initial state of the gel (Fig. 1A).

Fig. 1E shows the spectrum obtained when the tension of the silicone tube was released, compressing the gel. Again, quadrupolar splitting was evident in the spectrum with a value of 392 Hz and $\Delta\nu_{1/2} = 11.5$ Hz. The quadrupolar splitting was 0.48 times the value of the corresponding longitudinally stretched state (Fig. 1C).

RBCs were incorporated into a gelatin solution at 42 °C and then drawn into a silicone tube. The resulting ^{2}H NMR spectrum had a single Lorentzian line that was broader than in the absence of the RBCs (e.g., Fig. 1A), $\Delta\nu_{1/2} = 18.0$ Hz. The sample was then stretched to twice its original length and the resulting ^{2}H NMR spectrum had three broad Lorentzian signals. Based on the spectra above and from knowledge of the *Ht* of the RBC suspension used to form the sample, the central resonance was assigned to HDO inside the RBCs. Since the central resonance was not fully resolved from the quadrupolar doublet, numerical deconvolution was used to estimate resonance areas; it yielded a ratio of HDO outside to inside the cells of 6.3:1. By making a correction of 0.717 for the cell space that is available to water in isovolumic human RBCs [27,28] this corresponded to a final *Ht* of 19%. The values of $\Delta\nu_{1/2}$ obtained from the deconvoluted spectrum were, 49, 46, and 49 Hz, respectively.

Table 1
Summary of ^{2}H NMR data for gelatin-blood water exchange

Sample	T (°C)	Ratio of gel:blood	Extension factor[a]	Quadrupolar splitting (Hz)	$\Delta\nu_{1/2}$ (Hz)[b]	k_{-1} (s^{-1})		
						Matrix[c]	Initial rate[d]	Saturation transfer[e]
1 (100% D_2O)	15	5.4	1.0	452	73, 85, 74	38.5 ± 2.8	18.1± 0.2	—
	25	5.0	1.0	264	41, 102, 44	50[f]	36[f]	—
2 (100% D_2O)	15	—	0	0	12	—	—	—
		4.2	1.0	399	74, 80, 75	29.0 ± 2.5	19.2 ± 0.9	—
3 (20% D_2O)	15	6.4	1.0	388	56, 77, 65	31.7 ± 3.6	17.7 ± 0.3	30 ± 2
4 (20% D_2O)	15	—	0	0	46	—	—	—
		5.5	1.0	439	69, 73, 68	—	—	38 ± 1
5 (20% D_2O)	15	—	0	0	15	—	—	—
		6.3	1.0	336	49, 46, 49	—	—	37 ± 2

[a] Increase in length relative to the original length.
[b] From high to low frequencies.
[c] Matrix: k_{-1} at $t_m = 0$, 2D EXSY analysis, double exponential function, see Fig. 4.
[d] Initial rate approximation: This approach only extracts volumes from 2D EXSY spectra at small mixing times (between 10 and 100 ms) arising from the signal of the blood HDO molecules (as if that resonance was selectively irradiated by a soft 180° pulse [26]).
[e] Saturation transfer: see Fig. 2B.
[f] Based on three experiments only.

^{2}H NMR spectra of samples with RBCs in the gel were acquired on numerous occasions (see Table 1) and the three signals seen in Fig. 1F were very reproducibly obtained on stretching the gels. As with pure gelatin [18], the resonance separations increased linearly with the extent of stretching the gels. However, the magnitude of the quadrupolar splitting was less when a gel at 15 °C was heated to 25 °C (sample 1, Table 1): specifically, with 100% ^2H_2O, 30% (w/v) gelatin, extent of stretching twofold, and a final *Ht* ~22%, the splitting at 25 °C was 0.6 of that at 15 °C.

3.2. Saturation envelope

RF radiation was applied to the sample used for Fig. 1A, at the central frequency of the singlet, with sufficient power to suppress the whole resonance. This same power was then used in acquiring a large series of spectra with the irradiation applied across a range of ±700 Hz from the central frequency of the singlet. Plotting the combined area of all signals as a function of the off-set frequency yielded the graph (filled black squares) shown in Fig. 1A. Very similar saturation envelopes were obtained for the samples that gave the spectra in Fig. 1D and F, noting that the latter sample contained RBCs.

A remarkable finding is evident in the saturation envelopes for the stretched samples, such as Fig. 1B, C, and E. Peak suppression was not maximal when the saturating RF radiation was applied at the frequency of either of the quadrupolar signals, but it was maximal at the frequency of the original singlet, but even there full suppression was not obtained. Also, the central inverted spike was much narrower than for the unstretched-gel samples. Even though the radiation was applied in the frequency range between the two signals, no peak suppression occurred until near the edges of the resonances; and even when the radiation was applied directly at the frequency of the maximum amplitude of either signal, less than 20% suppression occurred. In other words, by far the most efficient peak suppression (saturation of magnetization) occurred when the radiation was applied at a frequency exactly mid way between the two quadrupolar signals. This phenomenon was generally observed in ^{2}H saturation transfer experiments.

In conclusion, saturation transfer was observed upon selective RF irradiation at the frequency mid-way between the two HDO resonances in stretched gelatin, independent of the presence of RBCs. But the shape of the saturation envelope was markedly altered in a systematic way by the presence of RBCs; this difference formed the basis of the following analysis of HDO transmembrane exchange. The inset in Fig. 1 illustrates the three main saturation envelopes: unstretched, black curve; stretched, red graph and; stretched in the presence of RBCs, brown curve.

3.3. Saturation transfer

Maximal peak suppression occurred when applying saturating RF irradiation at the mid-frequency between the two quadrupolar-split components of the extracellular HDO in stretched gels, with or without the presence of RBCs (Fig. 1 graphs). This meant that conventional saturation transfer analysis could not be applied to the gel-RBC system to measure the rate of transmembrane exchange of water. The outcome was equivalent to saturation 'spill-over' from one resonance/population to another that bedevils conventional saturation-transfer analysis. But because the inverted spike in the saturation envelope for extracellular HDO was so narrow (e.g., Fig. 1 inset: red graph) it was possible to use a range of saturation frequencies that were off-set from the central frequency, and thus

Table 2
NMR longitudinal relaxation times of ^2H spins in HDO in gelatin gels of three different compositions (all contained 20% D_2O), and three different extents of stretching

Sample	Extension factor[a]	Quadrupolar splitting (Hz)	$T_1^E \pm$ SD[c] Resonance 1[b]	$T_1^I \pm$ SD Resonance 2	$T_1^E \pm$ SD Resonance 3
30% (w/v) gelatin	0	0	139.9 ± 0.17	—	
	1.0	303	138.7 ± 0.62	—	138.6 ± 0.52
	1.5	407	138.3 ± 0.50	—	138.0 ± 0.40
50% (w/v) gelatin	0	0	106.9 ± 0.12	—	
	1.0	466	106.4 ± 0.22	—	106.2 ± 0.21
	1.5	652	104.5 ± 0.57	—	104.4 ± 0.49
30% (w/v) gelatin + 18% RBCs	1.0	465	90.5 ± 0.45	86.6 ± 0.85	90.2 ± 0.57
	1.5	626	90.5 ± 0.95	86.5 ± 0.84	90.4 ± 0.96
			30.9 ± 1.5	Saturated	30.0 ± 1.2
			28.4 ± 0.81	Saturated	27.8 ± 0.50

[a] Increase in length relative to the original length.
[b] Labelling of resonances was from high to low frequency.
[c] Denotes standard deviation, which along with mean values was estimated by nonlinear regression (see Section 2.6).

to saturate the intracellular magnetization while not affecting to a large extent the extracellular magnetization. Therefore, relaxation of the requirement to fully saturate the magnetization of the intracellular HDO, because its central frequency could not be used without suppressing the extracellular resonances, required our modified saturation transfer theory to estimate k_{-1} (Theory section). An important point about this analysis, that distinguishes it from that applied to chemical exchange, that cannot be 'switched off', is that the T_1^E of HDO in the pure extracellular medium was able to be measured independently of the exchanging system containing RBCs.

Table 2 shows that in samples of gelatin alone the T_1^E decreased with an increase in gelatin concentration. Decrease was also evident in samples that contained RBCs for both the intra- and extracellular HDO due to exchange between pools (data series not shown); but remarkably, stretching these gels had no significant effect on the estimates of T_1^E or T_1^I (shown for 30% gelatin in the last section of Table 2); and the values of T_1^E were always greater than T_1^I. When the intracellular HDO magnetization was saturated the corresponding $T_{1,sat}^E$ was $\sim 1/3$ of T_1^E. With conventional saturation transfer experiments this difference would normally be taken as direct evidence of exchange between the two sites, but because of the peculiar effect of resonance suppression by RF radiation at the central frequency this could not be concluded without further consideration, as follows.

Fig. 2 shows the ^2H NMR spectrum obtained from HDO in RBCs and their surrounding medium in stretched-gelatin gel (as in Fig. 1G); note that the intracellular HDO resonance was almost fully resolved from the other two. Numerical deconvolution was applied to this control spectrum and also from a series of spectra obtained when saturating RF radiation was applied over a range of frequencies, off-set from the central frequency. The saturation envelopes for both the intra- and extracellular HDO had distinct minima at the central frequency (as in Fig. 1) but the central inverted spike was much more pronounced for the extracellular HDO than for the intracellular resonance. The data set in Fig. 2B with the ω-shaped profile (solid triangles) is the values of k_{-1} estimated with $T_1^E = 139$ ms (Table 1) using the analysis given in the Theory section. The estimate of k_{-1} was invalid at an off-set frequency of 0.0 Hz since the magnetization of both spin populations were maximally saturated. Information on HDO exchange, expressed in the extent of saturation transfer, was most apparent in the regions of the graph where the extracellular HDO saturation envelope was effectively a plateau and also where there was concomitant suppression of the intracellular HDO resonance; this was when the RF radiation was centred on the region of the envelope from ± 30 to ± 45 Hz. Therefore, from this experiment the value of k_{-1} was estimated to be $37 \pm 2\ s^{-1}$. Repeated experiments gave similar rate constants (Table 1). In order to compare and validate the results obtained with this method we sought an alternative way to measure these rate constants, and this is explained next.

3.4. 2D EXSY

Fig. 3A shows an oblique image of the 2D EXSY spectrum obtained with a very small mixing time ($t_{mix} = 1$ ms) from a stretched-gel sample (sample 1) that consisted of 30% (w/v) gelatin with RBCs suspended in it. The inset in Fig. 3A shows the corresponding contour plot. Five signals are evident: the three signals in the leading diagonal are those seen in Fig. 2; the two symmetrically arranged cross peaks represent coherences between the two extracellular-HDO resonances.

The 2D EXSY spectrum shown in Fig. 3B was obtained from the same sample as used for Fig. 3A, but with $t_{mix} = 75$ ms. Nine signals are evident: the same five as for Fig. 3A with the cross peaks now having smaller intensities relative to the two main diagonal signals; the central intracellular-HDO resonance is diminished in relative intensity; and there are four additional cross peaks between the intra- and extracellular HDO signals. The inset in

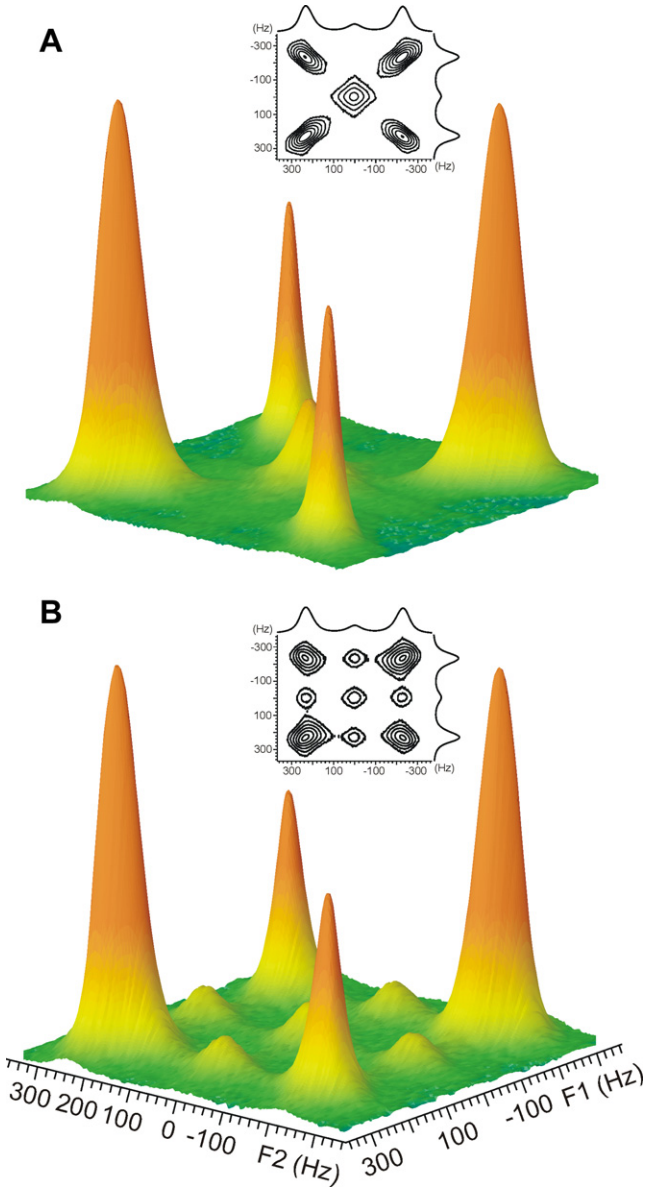

Fig. 3. ^{2}H NMR (61.422 MHz) 2D EXSY spectra of human RBCs, in gelatin stretched to twice its original length. (A) Oblique view of a spectrum acquired with $t_{mix} = 1$ ms, showing the two most prominent resonances assigned to extracellular HDO; the central resonance from HDO inside the RBCs; and the two 'cross' peaks from double quantum coherence between the two extracellular spin-populations. (B) Oblique view of a spectrum acquired with $t_{mix} = 75$ ms. The spectrum was scaled to give the largest diagonal signal the same amplitude as in (A); note the additional four 'cross' peaks between the two extracellular leading diagonal signals and the intracellular, central, HDO resonance. The insets show contour plots of each oblique spectrum. The sample temperature was 15 °C. NMR parameters: the 2D EXSY spectra were acquired with a full 16-step phase cycle; 64 increments in F1; and 990 points in F2; the free induction decays were Fourier transformed after applying a line-broadening factor of 3 Hz in F2; number of transients per spectrum, 32 (A) and 96 (B); resonance integrals were obtained from contour plots by using the manual integration routine in Topspin 2.0 (Bruker).

Fig. 3B shows the corresponding contour plot. It is the cross peaks that convey palpable evidence of the bi-directional flux of water across the RBC membranes.

Estimates of the values of the exchange rate constants were made with the back transformation analysis used for 2D EXSY spectra and the initial rate approximation [26] (Theory section). The relative peak volumes were measured by using three different approaches: (1) conventional delineation of the boundaries of peaks, where they were resolved from each other, or making a judgement on the cut-offs between signals; (2) automated volume estimation in Top Spin (Bruker); and (3) automated deconvolution followed by volume estimation of the fitted spectra, in Top Spin (Bruker). Based on comparing integrals from spectra obtained with small values of t_{mix} and the corresponding 1D equilbrium spectrum it was seen that the most robust estimates (in a statistical sense) were obtained by using the first method. Thus peak volumes in spectral matrices ($\mathbf{M}$ and $\mathbf{M}_0$ in the Theory section) were subjected to back-transformation analysis for a range of values of t_{mix}, in a program of six lines, written in *Mathematica* [24].

Fig. 4 shows a graph of the estimates of the efflux rate constant, k_{-1}, for HDO from RBCs at 15 °C, versus the corresponding value of t_{mix} used in the 2D EXSY experiment. A curious and obvious feature of the plot is its non-linearity. It was clear that the relationship between t_{mix} and k_{-1} was well described by a single exponential function. Importantly, extrapolation to $t_{mix} = 0$, of the curve for the combination of the data sets from three different samples (Table 1) gave a value of $k_{-1} = 31.5 \pm 2.2\ s^{-1}$. The individual extrapolation curves for the different gels yielded efflux rate constant values, k_{-1}, between 29 and 39 s^{-1},

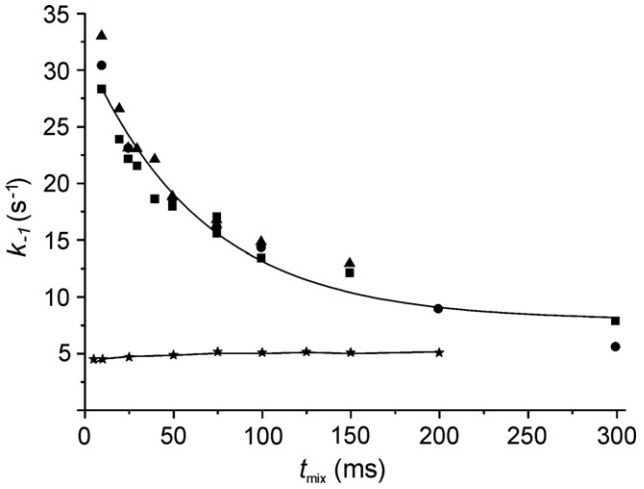

Fig. 4. Dependence of the estimate of the efflux rate constant, k_{-1}, for HDO (or ^2H_2O) in RBC suspensions in stretched gelatin-gel, on the value of t_{mix}, estimated by the matrix method from 2D EXSY spectra like Fig. 3. The solid triangles were data from sample 1 (Table 1). The solid squares were data from sample 2. The solid discs were data from a sample 3. The stars denote estimates of k_{-1} for exchange of the ^{2}H between the –O^{2}H of phenol and ^2H_2O obtained from ^{1}H NMR 2D EXSY spectra of a solution of phenol in $CHCl_3$ that contained ^2H_2O in approximately equal molar ratio with phenol. Note the similar values of k_{-1}, over a large range of values of t_{mix}. The temperature of all samples was 15 °C. Values for the fitted graphs are contained in Table 1.

whereas the initial rate approximation gave rate constant values around 18 s^{-1} (Table 1).

The 2D EXSY experiment was carried out at 25 °C for $t_{mix} = 10$, 25 and 50 ms. The estimated values of k_{-1} were 40.3, 31.5, and 25.0 s^{-1}, respectively. These values compare with the values obtained for the same gel when $T = 15$ °C of 32.6, 22.8, and 18.5 s^{-1}, respectively. If the values obtained at 25 °C are extrapolated to $t_{mix} = 0$ ms, a prediction for the rate constant of ~50 s^{-1} was found.

To explore if the observed dependence of k_{-1} on t_{mix} was a result of an artefact introduced by matrix manipulations, we performed 2D EXSY analysis on a model system using ^{2}H NMR. The sample consisted of phenol–O*D* (5% w/v) in $CHCl_3$ that contained ^2H_2O of sufficient amount to give a spectral resonance that was approximately the same intensity as that of the phenol–O*D*. The subsequent 2D EXSY spectrum contained cross peaks between the D_2O and the –O*D* signals; and the mathematical analysis of this 2-site system by the matrix method (Theory section) yielded estimates of the forward-exchange rate constant that were independent, within experimental error, of t_{mix}. The results are shown as the stars in Fig. 4. Analysis by the initial rate approximation gave very similar values of the rate constants.

4. Discussion

4.1. Quadrupolar splitting of HDO

All NMR methods that have been developed to measure membrane transport in cells rely on there already existing, or experimentally constructing, differences in one or more NMR parameters that apply between the inside and outside of the cells e.g., [17]. Our discovery of the very large quadrupolar splitting for HDO in contact with the stretched gelatin gel, as opposed to the singlet for HDO inside the cells (Fig. 1), affords a novel means of measuring water transport in RBCs. Applications to studying the kinetics of more slowly exchanging deuterated solutes seem to be possible. A time-series of spectra could be acquired, exploiting the quadrupolar-split outside the cells but not inside, to monitor changes in concentration of the solute inside or outside the cells.

4.2. Saturation envelope

A striking finding was that saturation of magnetization, and hence peak suppression, occurred when irradiation was applied at a frequency exactly between the two signals of the quadrupolar split HDO resonance. This occurred even in the absence of RBCs. The explanation for this effect is that stretching the gelatin-gel imparts structural anisotropy that invokes anisotropy of the average electric field-gradient tensor. The ^{2}H spins of HDO with their electric quadrupole moment are in rapid exchange between the bulk aqueous phase and in a transient way with the inhomogeneous electric fields. Consequently, the resonances of each of the two components of the quadrupolar doublet are the result of the weighted average of the zero-splitting chemical shift and that of the full quadrupolar coupling, which is of the order of kilohertz. Only a minute fraction of spins are at any moment in the presence of the ordered (in the *z*-direction) inhomogeneous electric fields while the vast majority are in the bulk medium. Therefore, this is an exchanging system, and saturation of magnetization at the zero-splitting chemical shift will be transferred by diffusive exchange to the whole system, thus giving resonance suppression in the spectrum.

4.3. Saturation transfer

A conventional analysis of saturation transfer spectra, to quantify the efflux rate of HDO from RBCs, was not possible. This was because of what amounted to an extreme 'power spill over' when attempting to saturate the magnetization of the intracellular HDO spin population. The mechanism of the spill over was itself an exchange phenomenon as explained above. The sharpness of the cut off of this effect (Figs. 1 and 2) when RF irradiation was applied a few Hz away from the central frequency, meant that at least an initial estimate could be made of k_{-1}. However, there was sufficient uncertainty in being able to reproducibly define the form of the saturation envelope without many experiments that an alternative approach was sought. Notwithstanding the greater complexity of setting up the experiment, the estimate of k_{-1} was close to those estimated by the Mn^{2+} doping method [1]. On the other hand the saturation transfer experiment is valuable for gaining an initial impression of whether an exchanging system will be amenable to a full 2D EXSY analysis.

4.4. 2D EXSY

The method that yielded more reliable estimates of the exchange of HDO across RBC membranes used 2D EXSY spectra; this method is established as being statistically robust [20].

The values of the efflux rate constant k_{-1} at $t_{mix} = 0$, 31.5 ± 2.2 s^{-1} indicated that the total water contents of the RBCs turned over ~30 times a second. This was less than but of the same order of magnitude as values already reported for human RBCs [1] in the temperature range 15–42 °C. The corresponding mean residence time, τ_e, at 15 °C is 32 ± 3 ms. Linear extrapolation of the limited data obtained at 25 °C would underestimate the value of k_{-1} but nevertheless the estimate of ~50 s^{-1} implies a value of τ_e of ~20 ms which is twice the generally accepted value of ~10 ms at 25 °C [1].

The causes of the under estimates of k_{-1} are possibly: (1) imperfect extrapolation to a value when $t_{mix} = 0$. Data for only three different mixing times were obtained at 25 °C. This may be clarified with a greater number of experiments, with smaller values of t_{mix}. (2) The high viscosity of the gelatin-gel could cause HDO that is involved in transmem-

brane exchange to be from a 'pool' that is close to the outside of the RBC membrane. In other words, with larger values of t_{mix}, more of the HDO would participate in the exchange but its diffusion is from a greater mean-distance and its mobility is retarded by the high viscosity of the medium. Hence experiments with increasing packing densities of RBCs should reveal an upward trend in the estimates of k_{-1} at a given value of t_{mix}. (3) Chemical interactions between gelatin and the RBC membrane could potentially interfere with the function of membrane transporters. This idea could be studied by measuring transmembrane exchange of species other than HDO, such as those that enter the RBC by a route other than aquaporins e.g., [7].

4.5. Further comparison with other methods, and caveats

The lack of requirement for a paramagnetic relaxation-enhancement cation such as Mn^{2+} [1,3–5] means that ions that potentially interfere with the water transporters are avoided and the sample remains stable and free of leakage of such ions for many hours. Thus the present method enables long (hours) metabolic time courses to be recorded while having the ability to periodically measure (changes in) water transport rate that may be modulated during the incubation.

Another advantage of the new method is the lack of a background ^1H envelope of resonances assigned to non-exchangeable protons on cellular proteins; these potentially interfere with quantifying the ^1H_2O resonance intensity.

Disadvantages are: (1) the requirement to conduct the measurements at a temperature below the melting temperature of the gel, which is ~28 °C. The principles of the method are generic, so if a higher melting-temperature gel, that is compatible with cells, emerges it could be used to study HDO exchange at higher temperatures. (2) There is a potential problem with using isotopes when studying kinetic events in cells. And it is known that the exchange rate of ^2H_2O in human RBC is less than for pure ^1H_2O [29]. However, in the present work usually only 20% of the water was labelled with ^2H, so under these circumstances the correction applied to k_{-1} to make it apply to pure ^1H_2O would be a factor of ~1.1; this is within the SD, of the mean-estimates. (3) The requirement to suspend the cells in liquid gelatin means that sample-preparation time is greater than for some of the other membrane transport methods; on the other hand the stretching of the cells in a gel provides scope for other types of biophysical analyses of cells in anisotropic media.

4.6. Future directions

Although it was possible to extrapolate the fitting function in Fig. 4 to obtain a consistent (with other methods) estimate of the efflux rate constant for HDO in RBCs, the physical basis of the dependence of the estimate of k_{-1} on t_{mix} for the Matrix method in the 2D EXSY experiment is, as yet, unknown. The intensities of the cross-peaks are less than they should be if there was no dependence of the estimate of k_{-1} on t_{mix}. This suggests that exchange of quadrupolar spins involves loss of phase coherence that is not accounted for in the simple 2-site Bloch–McConnell theory used here to analyse the data; and only in the limit of $t_{mix} \to 0$ does this simple theory apply. Reports on exchange involving quadrupolar nuclei especially in the solid state have appeared over many years e.g., [30,31] but there seem not to be any on ^2H exchange in aqueous solutions. Physical understanding from this previous work will probably be needed to solve the problems raised.

5. Conclusions

A large ^2H NMR quadrupolar splitting of the HDO resonance in stretched-gelatin gels added another NMR parameter to those that can be exploited in studies of membrane transport in cells. The use of the ^2H nucleus avoids interfering signals from other species rich in ^1H, ^{13}C or ^{31}P. By using different NMR techniques (saturation transfer and 2D EXSY) we were able to reproducibly obtain efflux rate constants close to those already published. The saturation transfer analysis was complicated by a peculiar response of the quadrupolar-exchange system to saturating RF radiation, whereas the matrix method of the 2D EXSY experiments yielded estimates of k_{-1} that depended on the experimental parameter t_{mix}. The physical basis of this dependence is unexplained at this stage, and the finding urges further investigation. Applications to cells other than RBCs are also anticipated.

Acknowledgments

The work was supported by a Discovery Grant from the Australian Research Council to P.W.K. Drs. Bob Chapman and David Philip are thanked for early NMR input and discussions on quadrupolar-spin systems. Dr. Bill Bubb is thanked for assistance with the NMR spectrometer and valuable discussions.

References

[1] Gh. Benga, Prog. Biophys. Molec. Biol. 51 (1988) 193–245.
[2] P.W. Kuchel, Gh. Benga, Biosystems 82 (2005) 189–196.
[3] Gh. Benga, V.I. Pop, O. Popescu, V. Borza, Biosci. Rep. 10 (1990) 31–36.
[4] Gh. Benga, B.E. Chapman, C.H. Gallagher, D. Cooper, P.W. Kuchel, Comp. Biochem. Physiol. 104A (1993) 799–803.
[5] M.D. Herbst, J.H. Goldstein, Am. J. Physiol. 256 (1989) C1097–C1104.
[6] J. Kärger, H. Pfeifer, W. Heink, Adv. Magn. Reson. 12 (1988) 1–89.
[7] A.R. Waldeck, P.W. Kuchel, A.J. Lennon, B.E. Chapman, Progr. NMR Spectrosc. 30 (1997) 39–68.
[8] B.E. Chapman, P.W. Kuchel, Diff. Fund. 4 (2007) 8.1–8.15.
[9] C. Gasparovic, N.A. Matwiyoff, Magn. Reson. Med. 26 (1992) 274–299.

[10] S.C.K. Chu, Y. Xu, J.A. Balschi, C.S. Springer, Magn. Reson. Med. 13 (1990) 239–262.
[11] C.S. Springer, NMR Biomed. 7 (1994) 98–202.
[12] J.G. Li, G.J. Stanisz, R.M. Henkelman, Magn. Reson. Med. 40 (1998) 79–88.
[13] D.J. Philp, W.A. Bubb, P.W. Kuchel, Magn. Reson. Med. 51 (2004) 441–444.
[14] E. Bruno, G. Digilio, C. Cabella, A. de Reggi, S. Baroni, V. Mainero, S. Aime, Magn. Reson. Med. 56 (2006) 256–265.
[15] T. Larkin, W.A. Bubb, P.W. Kuchel, Biophys. J. 92 (2006) 1770–1776.
[16] T.R. Brown, Phil. Trans. Roy. Soc. Lond. B 289 (1980) 441–444.
[17] P.W. Kuchel, NMR Biomed. 3 (1990) 102–119.
[18] P.W. Kuchel, B.E. Chapman, N. Müller, W.A. Bubb, D.J. Philp, A.M. Torres, J. Magn. Reson. 180 (2006) 256–265.
[19] C. Naumann, W.A. Bubb, B.E. Chapman, P.W. Kuchel, J. Am. Chem. Soc. 129 (2007) 5340–5341.
[20] P.W. Kuchel, B.T. Bulliman, B.E. Chapman, G.L. Mendz, J. Magn. Reson. 76 (1988) 36–142.
[21] B.T. Bulliman, P.W. Kuchel, B.E. Chapman, J. Magn. Reson. 82 (1989) 132–138.
[22] H.M. McConnell, J. Chem. Phys. 28 (1958) 430–431.
[23] K. Kirk, P.W. Kuchel, J. Magn. Reson. 68 (1986) 311–318.
[24] S. Wolfram, The *Mathematica* Book, Version 6, Wolfram Media (2007) Champaign, IL.
[25] J.V. Dacie, S.M. Lewis, Practical Haematology, Churchill Livingstone, (1975) Edinburgh.
[26] A. Kumar, G. Wagner, R.R. Ernst, K. Wüthrich, J. Am. Chem. Soc. 103 (1981) 3654.
[27] J.E. Raftos, B.E. Chapman, P.W. Kuchel, V.A. Lovric, I.M. Stewart, Haematologia 19 (1986) 251–268.
[28] J.E. Raftos, B.T. Bulliman, P.W. Kuchel, J. Gen. Physiol. 95 (1990) 1183–1204.
[29] Gh. Benga, V. Morariu, B.E. Chapman, P.W. Kuchel, Bull. Molec. Med. 15–16 (2003) 35–41.
[30] C. Hall, D.W. Kydon, R.E. Richards, R.R. Sharp, Proc. Roy. Soc. Lond. A 318 (1970) 119–141.
[31] R.W. Shurko, S. Wi, L. Frydman, J. Phys. Chem. 106 (2002) 51–62.